A Dynamic Model of Synthetic Resting-State Brain Hemodynamics

Rashid Ghorbani Afkhami*, Kathy Low†, Frederick Walker‡ and Sarah Johnson*
*School of Electrical Engineering & Computing
University of Newcastle, Callaghan, NSW, Australia
Email: rashid.ghorbaniafkhami@uon.edu.au, sarah.johnson@newcastle.edu.au
†Beckman Institute
University of Illinois, Urbana, Illinois, USA
Email: lowka@illinois.edu
‡School of Biomedical Sciences
University of Newcastle, Callaghan, NSW, Australia
Email: rohan.walker@newcastle.edu.au

***Abstract*—Near infrared spectroscopy (NIRS) is an emerging field of brain study. From an engineering perspective, the absence of a ground truth signal or a model for producing synthetic data has hindered understanding of the underlying elements of this signal and validating of existing algorithms. In this paper, a dynamic model of artificial NIRS signal is proposed. The model incorporates arterial pulsations, its possible frequency drifts, Mayer waves, respiratory waves and other very low frequency components. Parameter selection and model fitting has been carried out using measurements from a NIRS database. To be general in the process of parameter selection, our dataset included 4 NIRS devices and 256 channels for each subject, covering all the scalp and therefore providing realistic measures of the varying parameters. Results are compared with the real data in time and frequency domains, both showing high level of resemblance.**

***Index Terms*—near infrared spectroscopy, synthetic signal, brain hemodynamics**

I. Introduction

Near infrared spectroscopy (NIRS) is an emerging field of brain study. It uses the near infrared (690nm to 900nm) portion of the electromagnetic spectrum to emit light into the brain. The light is scattered and a very small portion (approximately one out of 10^9 photons) finds its way to the light detectors placed $2-4$cm away from the source [1]. Over this spectrum light is mainly absorbed by oxygenated and deoxygenated blood which have different absorption coefficients. Therefore, using at least two wavelengths one can separate these chromophores as indicators of brain activation [1]. NIRS has several advantages compared to other methods of brain study. Low cost, portability and high temporal resolution are the features making NIRS a worthy alternative to the well-known functional magnetic resonance imaging (fMRI). NIRS also offers higher spacial resolution than electroencephalography (EEG), allowing regional studies. NIRS has already found its place in scientific research into cerebrovascular disease, cerebral arterial pulsation, functional connectivity, brain computer interface and event-related fast optical signals [2]–[4].

Depending on the application, various signal processing procedures are adopted to extract solely the desired signal. This process would benefit from knowledge of all NIRS signal components including instrumental noise, arterial pulsation, hemodynamic response, respiratory waves, Mayer waves and motion artifacts [4], [5]. Currently, new biomedical signal processing algorithms are generally evaluated using data from only a few participants and with a fixed instrumental setting. In addition, rarely any database is available for more comprehensive signal processing studies. Therefore, realistic artificial NIRS signals can facilitate the evaluation of these algorithms.

In this paper, we present a novel model for generating artificial NIRS time series which has the same time and frequency features as the real intensity-normalized NIRS signals. The model encompasses arterial pulsations, instrumental noise and low frequency components. By adjusting the mean and standard deviation of the heart rate, sampling frequency and also frequency-domain features like power ratio of different bandwidths, proposed model can simulate realistic NIRS signals.

II. Signal Modeling

In this section we present the elements of the proposed model and how they are combined. Throughout the paper, any signal from real NIRS measurements will be noted by a superscript check e.g., $\check{s}$.

Our proposed model describing the NIRS signal encompasses the following components,

$$\mathrm{s} = \begin{bmatrix} \mathrm{a_{AP}} & \mathbf{1} & \mathrm{a_{LF}} \end{bmatrix} \begin{bmatrix} \mathrm{s_{AP}} \\ \mathrm{s_{GN}} \\ \mathrm{s_{LF}} \end{bmatrix} + \mathbf{1}. \tag{1}$$

Where s is the NIRS time series vector formed with the arterial pulsation signal, $\mathrm{s_{AP}}$, additive white Gaussian noise, $\mathrm{s_{GN}}$, and low frequency components, $\mathrm{s_{LF}}$. $\begin{bmatrix} \mathrm{a_{AP}} & \mathbf{1} & \mathrm{a_{LF}} \end{bmatrix}$ is the $N \times 3$ matrix of corresponding amplitudes, where N is the number of realizations. $\mathbf{1}$ is a $N \times 1$ vector of ones. Typically, experimental NIRS data is normalized to a mean of 1 and we

ISBN 978-90-827970-1-5 © EURASIP 2018

do the same in this model. N is selected based on the desired sampling frequency, f_s, and signal length in seconds.

A. Arterial Pulsation Signal

Arterial pulsations (AP) are the most distinguishable components in the NIRS signal with high power. These signals are the footprint of massive changes in blood volume as the heart pumps and blood is forced into cerebral arteries. This volume of blood absorbs a larger portion of the optical signal and a decrease of detected light intensity becomes evident. AP signals are used to extract pulse transit time and cerebrovascular compliance in order to assess cerebral arterial health [4]. There are several factors such as the environment temperature, body position, emotional state, exercise and medicine use that can alter the heart rate. In our model we assume a stationary participant with no change in these factors. However, two key elements continuously influence the heart rate. It is known that heart rate accelerates during inspiration and slows down during expiration. This phenomenon is referred to as respiratory sinus arrhythmia (RSA) [6]. In addition, Mayer waves, for which the cause is debatable, result in small frequency drifts in the electrocardiogram (ECG) signal [7]. Due to the same nature of AP signals in ECG and NIRS, we assume that these frequency drifts are also present in the NIRS signals.

We define $\mathrm{s_{AP}}(n)$ as a sinusoidal with a time-varying instantaneous frequency function, $f(n)$, and random phase, ϕ_0. That is,

$$\mathrm{s_{AP}}(n) = \sin\left[2\pi \sum_{i=0}^{n} \left(H_{\text{mean}} + H_{\text{std}} f(i)\right) + \phi_0\right]. \quad (2)$$

Where H_{mean} and H_{std} are the heart rate mean and standard deviation in Hertz, respectively. To model the mentioned frequency drifts, we use a similar concept to the "RR interval" used in the ECG signal analysis. R peaks are the most distinguishable peaks in the ECG signal and RR peak-to-peak intervals are defined as the time between consecutive R peaks. Similarly, we define $p(n)$ as the instantaneous frequency at time n (which can be estimated in a real signal by measuring the peak-to-peak interval in a local window around time point n). Now, Respiratory and Mayer drifts can be modeled based on a previously established method proposed to produce synthetic electrocardiograph (ECG) signals [7]. The power spectrum of $p(n)$ is described with two components as,

$$P(f) = \sum_{i=1}^{2} \frac{c_i^2}{\sqrt{2\pi\sigma_i^2}} \exp\left(\frac{(f-f_i)^2}{2\sigma_i^2}\right). \quad (3)$$

Where f_i, σ_i and c_i represent the center frequency, standard deviation and power of the frequency drift, respectively of Mayer signal ($i = 1$) and respiratory signal ($i = 2$). Taking the inverse Fourier transform of $\sqrt{P(f)}$, using random phase, $p(n)$ is generated as,

$$p(n) = \{\mathcal{F}^{-1}\left[\sqrt{P(f)}e^{j\theta}\right], \quad \theta \backsim \mathcal{U}[0, 2\pi)\}. \quad (4)$$

Where $\mathcal{F}^{-1}$ is the inverse Fourier operator and $\mathcal{U}$ is the uniform distribution. For simplicity, the Fourier transform is always done with the sampling frequency of 10 and then the signal is up-sampled to the desired sampling frequency, f_s. Having the instantaneous period time series, $p(n)$, we calculate the time-varying frequency function as,

$$f(n) = \frac{1}{p(n)}. \quad (5)$$

$f(n)$ is then normalized to zero mean and unit variance to be used in (2).

B. White Gaussian Noise

NIRS signals usually contain high amounts of white Gaussian noise (WGN) originating from instruments in the measurement site. As the name suggests, WGN is characterized as uniformly distributed in the frequency domain and therefore it is easily detected in bandwidths which are clear from any other known components. This feature will be used to set the noise power. In mathematical terms,

$$\mathrm{s_{GN}}(n) \backsim \mathcal{N}(0, N), \quad (6)$$

where $\mathcal{N}$ is the normal distribution with zero mean and variance of N. An adequate amount of noise power, N, needs to be selected to obtain a realistic model. For this purpose, we use a power-ratio factor. Assuming a known power ratio over specific bandwidths of the final signal, N is increased until the desired ratio is reached.

First we define the power ratio function, Ψ, of two arbitrary discrete signals, x with length N and y with length of M as,

$$\Psi(x, y) = 10\log_{10}\left[\frac{\frac{1}{N}\sum_{n=1}^{N} x^2(n)}{\frac{1}{M}\sum_{n=1}^{M} y^2(n)}\right], \quad (7)$$

where Ψ is in decibels (dB).

Then, knowing the heart beat frequency, the AP signal is extracted with an infinite impulse response (IIR) bandpass filter with the bandwidth of 0.4Hz centered around the heart rate. The result is called w_{AP}. Another IIR filter is applied to the frequency band of 3-10Hz. Under the assumption that this spectrum contains only white Gaussian noise. The output signal is called w_{GN}. We define,

$$\psi_{\text{GN}} = \Psi(w_{\text{GN}}, w_{\text{AP}}). \quad (8)$$

Finally, to add sufficient amount of WGN, the noise power, N, is increased over an iterative process until,

$$\psi_{\text{GN}} = Q. \quad (9)$$

This strategy will help us implement realistic values for noise power.

C. Low Frequency Components

"Low frequency components" or "LF components" are more general terms used to refer to the two main elements of the NIRS signals. First, the Mayer and the respiration waves at around 0.1 and 0.25Hz. Second, the very low frequency (VLF) components at less than 0.1Hz.

ISBN 978-90-827970-1-5 © EURASIP 2018

1) Mayer and Respiratory Waves: These two elements are also present in NIRS signals as reported in the literature [5]. To clarify, in Section II-A, we mentioned the frequency drifts that these signals cause to the heart rate and here, we discuss the amplitude changes of NIRS signals caused by the same sources. Thus, we generate $p_1(n)$ as per (4) (with a different realization of θ), then normalize it to zero mean and unit variance. We define

$$\mathrm{s_{MR}}(n) = p_1(n), \tag{10}$$

which will be added to other low frequency components discussed in this section.

2) Very Low Frequency Components: Very low frequency, less than 0.1Hz, components of the NIRS signal correlate with similar components in blood-oxygenation level dependent (BOLD) functional magnetic resonance imaging (fMRI) data [8]. Although the source of these signals is unclear, they have thought to be associated with changes in vascular dilation, vaso-motion, and Mayer waves [8]. We take advantage of the correlation between VLF BOLD and NIRS by adopting signal processing approaches proposed in the literature to model the low frequency components in the BOLD signal [9].

The LF part of our synthetic model is defined as,

$$s_{\mathrm{LF}}(n) = s_{\mathrm{MR}}(n) + \sum_{k=1}^{K} A(k)\cos(2\pi\phi(k)n). \tag{11}$$

Where $\mathrm{s_{MR}}(n)$ represents Mayer and respiration amplitude changes. K is the number of VLF components. A is a $1 \times \mathrm{K}$ vector of amplitudes. $\phi(k) = f_1 + (f_2 - f_1)/(K-1).(k-1)$, with f_1 and f_2 being the low and high frequency limits of the VLF elements.

The final model of the synthetic NIRS signal depends on total of sixteen tunable parameters. Sampling frequency, six variables for constructing $P(f)$ in (3), heart rate parameters, Q for the Gaussian noise, four for determining K, A and ϕ in (11), and two amplitude parameters in (1). In the following we set realistic values for each of them.

III. Parameter Estimation

In this section we discuss the issue of proper parameter selection for our proposed model. For some variables, we have used the values suggested in the literature. However, for the others, a NIRS dataset has been used for the parameter selection.

A. Dataset

Our data consists of 5 adult participants for whom 30 seconds of baseline resting data were recorded. The setup montage consisted of 16 detectors each crossed with 16 time multiplexed sources (half of the sources operating at 690nm and half at 830nm), making total of 256 channels. Four frequency domain NIR spectrometers (ISS Imagent™, Champaign, Illinois) were operating simultaneously with the rate of 39.0625Hz for data acquisition.

Participants were recruited from the Champaign-Urbana community, were paid for their participation, and signed informed consent in accordance with the University of Illinois at Urbana-Champaigns Institutional Review Board.

B. AP Parameters (f_1,f_2,c_1,c_2,σ_1,σ_2,a_{AP},H_{mean},H_{std})

For the arterial pulsation signal, default values of mean and standard deviation of the heart rate are $H_{\mathrm{mean}} = 60$bpm (i.e., 1Hz) and $H_{\mathrm{std}} = 5$bpm (i.e., ~ 83mHz), respectively [7]. In (3), the Mayer waves are centered at $f_1 = 0.1$ and with the normal breathing rate of 12-18 breath per minute, f_2 is set to 0.25Hz [7]. The value of 0.029Hz have been chosen for the standard deviations σ_1 and σ_2 and the value of 0.029 have been chosen for the power factors c_1 and c_2 based on the measurements from the dataset.

The AP signal is the main component of our synthetic model, and other elements are normalized based on the AP. Therefore, the amplitude of this signal is set to the constant value of $a_{\mathrm{AP}} = 0.01$, based on the intensity-normalized data from the dataset.

C. WGN Variance and Q

As mentioned in Section II-B, the noise power will be tuned by the power ratio factor, Q. We have used our dataset to measure the same parameter for the real data. Assuming that $\check{w}_{\mathrm{AP}}$ and $\check{w}_{\mathrm{GN}}$ are formed from the real data with the same filtering process explained in Section II-B, we can calculate

$$\check{\psi}_{\mathrm{GN}} = \Psi(\check{w}_{\mathrm{GN}}, \check{w}_{\mathrm{AP}}). \tag{12}$$

$\check{\psi}_{\mathrm{GN}}$ will be the realistic values of Q in (9). Selecting channels with the optimum source/detector distance (i.e., 2 to 4cm, which account for the total of 594 channels), we fit a normal distribution, $\mathcal{N}(\mu, \sigma)$, to the measured $\check{\psi}_{\mathrm{GN}}$ values. The resulted distribution is $\mathcal{N}(-6.69, 7.27)$, which will be used to acquire realistic values for the power ratio parameter, Q.

D. LF Parameters (K, A, a_{LF})

Based of our simulations and visual validation of time domain and LF bandwidth in the frequency domain we have chosen the default value of 20 for the number of VLF components, K, in (11). The vector of amplitudes, A, has random numbers uniformly chosen from $[-1, 1]$. For Φ, f_1 and f_2 are set to 0.01Hz and 0.09Hz, respectively to cover the LF bandwidth up until the Mayer frequency.

In order to set a_{LF} as a realistic LF signal power in our model, we have used the power-ratio strategy of Section II-B. Using the dataset, an IIR bandpass filter is applied to the frequency band of [0.01-0.26]Hz (i.e., the LF band), producing $\check{w}_{\mathrm{LF}}$, then the power ratio for the low frequency signal is defined as,

$$\check{\psi}_{\mathrm{LF}} = \Psi(\check{w}_{\mathrm{LF}}, \check{w}_{\mathrm{AP}}), \tag{13}$$

Where $\check{w}_{\mathrm{AP}}$ is described in III-C. Having the realistic $\check{\psi}_{\mathrm{LF}}$ values from the optimally distanced source/detector pairs, we fit a normal distribution to these values. The resulted distribution is $\mathcal{N}(3.30, 11.51)$, which will be used to acquire realistic values for the power ratio parameter, ψ_{LF} (defined as (13) for the synthetic signal). After an appropriate value is set

ISBN 978-90-827970-1-5 © EURASIP 2018

TABLE I
MODEL PARAMETERS

Parameter		Literature	Dataset	Default
Device	f_s	—	39.0625Hz	User-defined
AP	f_1	100mHz	$[118, 110, 101, 108, 95]$mHz	100mHz
	f_2	250mHz	$[203, 180, 175, 203, 190]$mHz	250mHz
	c_1	$c_1^2/c_2^2 = 0.5$	$[26, 33, 20, 28, 42] \times 10^{-3}$	29×10^{-3}
	c_2		$[23, 33, 26, 25, 33] \times 10^{-3}$	29×10^{-3}
	σ_1	10mHz	$[13, 34, 25, 32, 38]$mHz	29mHz
	σ_2	10mHz	$[15, 38, 26, 32, 32]$mHz	29mHz
	a_{AP}	—	0.01	0.01
	H_{mean}	60bpm (1Hz)	$[61, 58, 89, 72, 62]$bpm	60bpm
	H_{std}	83mHz	$[55, 50, 70, 58, 68]$mHz	83mHz
WGN	Q	—	$\mathcal{N}(-6.69, 7.27)$	$\mathcal{N}(-6.69, 7.27)$
LF	K	—	20	20
	A	$\mathcal{U}[-1, 1]$	—	$\mathcal{U}[-1, 1]$
	f_1	0.01Hz	—	0.01Hz
	f_2	0.09Hz	—	0.09Hz
	ψ_{LF}	—	$\mathcal{N}(3.30, 11.51)$	$\mathcal{N}(3.30, 11.51)$

for ψ_{LF}, a non-linear least-squares minimization problem is solved to find the right a_{LF} for the LF components.

All the model parameters are summarized in Table I with the values suggested by the literature and the values measured from the dataset. The physiological values like the mean and standard deviation of the heart rate and Mayer and respiration frequencies measured from the dataset fall within their typical intervals suggested by the literature. However, the differences between the reported values for c_1, c_2, σ_1 and σ_2 of the AP signal are presumed to be the result of differences between ECG and NIRS. Thus, the default values for these parameters (last column of Table I) are based on the measurements from the dataset.

IV. Model Validation

Results of the proposed method for producing synthetic intensity-normalized NIRS signals are presented in this section. We compare the signal generated by the model with two real signals taken from our dataset. The model parameters have been set to default as mentioned in Table I, except the three values, Q, ψ_{LF} and heart rate that vary considerably among subjects or among the different channels of the same subject. These parameters are set to the same values derived from the real signal used for comparison. Fig. 1 (a) shows 15 seconds of resting state data from the dataset described in section III-A. Using the data shown in Fig. 1 (a), the parameters Q, $\check{\psi}_{\text{LF}}$ and heart rate were measured as -3.97dB, 4.18dB and 89bpm, respectively. Fig. 1 (b) is the 15-second sample of a synthetic signal formed using these values. Moreover, Fig. 1 (c) compares the two signals in the frequency domain. Another example is illustrated in Fig. 2, for which the parameters Q, $\check{\psi}_{\text{LF}}$ and heart rate were measured as 7.85dB, 20.35dB and 61bpm, respectively. The sampling frequency of the model is set to 39.0625Hz, same as the dataset. The results show that the outputs of the proposed model closely match the real measurements.

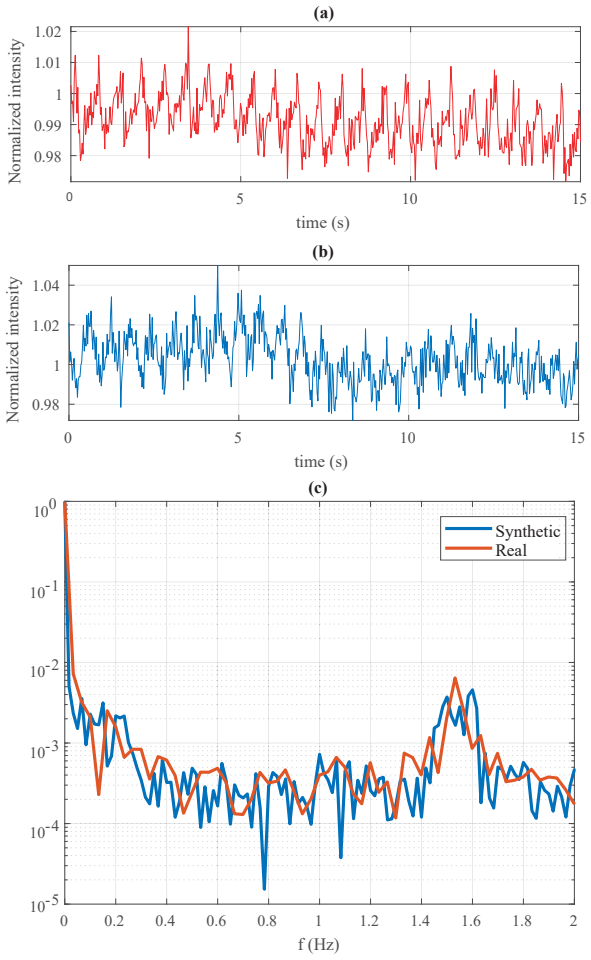

Fig. 1. (a) Sample from dataset: subject 3, 40mm source/detector distance, 830nm wavelength (b) synthetic signal (c) power spectrum.

V. Discussion

In order to model such complicated signals, assumptions should be made to simplify the process while holding the key features and components. Assumptions made in this paper are,

- The frequency drifts of the arterial pulsation signal have the same characteristics as the ECG-RR interval signal. This assumption holds firstly, based on the nature of the AP signal discussed in II-A and secondly, based on the analysis done by [4], [10] which have simultaneous ECG and NIRS measurements.
- The effect on signal amplitude of Mayer and respiratory amplitude changes can be modeled by a Gaussian function in the frequency domain. This assumption is based on the inherent natural behavior of the physiological phenomena. Similar assumption is made in [7] for modeling the frequency drifts of the same signal components.
- Mayer, respiratory and very low frequency waves can be combined into one component (i.e, the low frequency component) to be described with a single amplitude parameter, a_{LF}. Our data analysis show that a good level

ISBN 978-90-827970-1-5 © EURASIP 2018

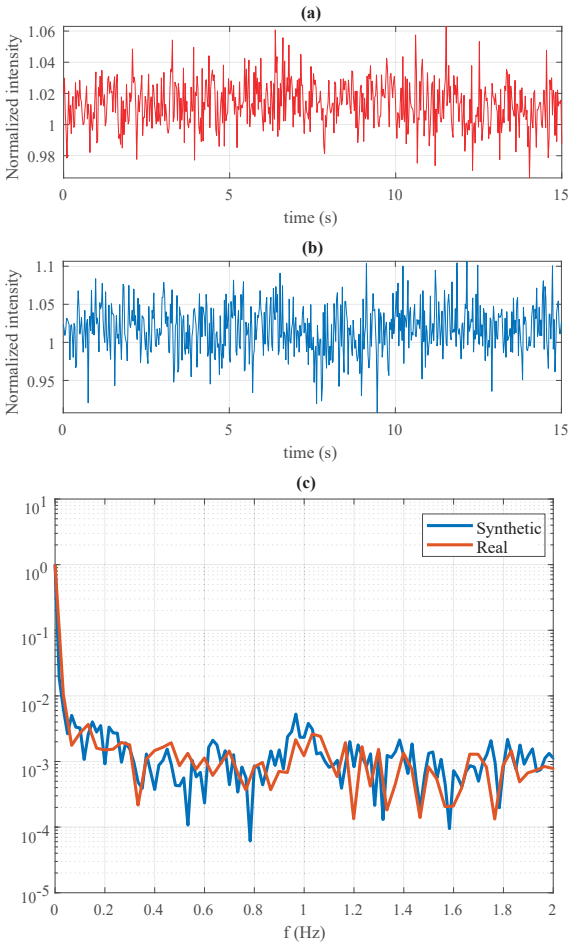

Fig. 2. (a) Sample from dataset: subject 1, 31mm source/detector distance, 690nm wavelength (b) synthetic signal (c) power spectrum.

of accuracy can be achieved with this method. However, simultaneous ECG, respiration and NIRS monitoring can help in better understanding of these components and possibly separating them.

- We have assumed that the frequency drifts and the amplitude changes caused by the Mayer and respiratory waves are not synchronized and therefore different realizations of θ in (4) have been used for each component. This assumption has been made since the nature of those components have not yet been explored for NIRS signals.

The hemodynamic response function indicates the oxy- and deoxy-hemoglobin responses in NIRS signals during certain cognitive tasks. The nature of this signal has been investigated thoroughly in the literature using data from functional MRI BOLD (blood oxygen level dependent), [11], [12] and NIRS, [13]. Therefore, synthetic hemodynamic response function can be easily added to the model to simulate a specific experimental paradigm; procedures are explained in literature [13], [14].

The current model is limited to only being tested by the ISS Imagent NIRS which is a frequency-domain device. A more comprehensive study would test and adjust the parameters to other frequency-domain or continuous wave devices.

VI. Conclusion

In this paper a novel method for generating synthetic NIRS signal is proposed. The model has low-frequency elements, arterial pulsations, Mayer and respiration waves. Appropriate default values based on the literature or probability distribution functions based on the real measurements have been proposed for deriving the required elements. Results of synthesized data are compared in time and frequency domain with the real NIRS measurements, which indicates the accuracy of the proposed model. The model can be used to investigate different signal processing algorithms proposed for NIRS data analysis.

References

[1] J. K. Choi, M. G. Choi, J. M. Kim, and H. M. Bae, "Efficient data extraction method for near-infrared spectroscopy (NIRS) systems with high spatial and temporal resolution," IEEE Trans. Biomed. Circuits Syst., vol. 7, no. 2, pp. 169-177, Apr. 2013.

[2] Hellmuth Obrig, "NIRS in clinical neurology a promising tool?," NeuroImage, vol. 85, part. 1, pp. 535–546, 2014.

[3] C. Tse, B. A. Gordon, M. Fabiani and G. Gratton, "Frequency analysis of the visual steady-state response measured with the fast optical signal in younger and older adults," Biological Psychology, vol. 85, no. 1, pp. 79–89, 2010.

[4] C. H. Tan, K. A. Low, T. Kong, M. A. Fletcher, B. Zimmerman, E. L. Maclin, A. M. Chiarelli, G. Gratton and M. Fabiani, "Mapping cerebral pulse pressure and arterial compliance over the adult lifespan with optical imaging," PloS One, vol. 2, no. 2, 2017.

[5] T. J. Huppert, S. G. Diamond, M. A. Franceschini, and D. A. Boas, "HomER: A review of time-series analysis methods for near-infrared spectroscopy of the brain," Appl. Opt., vol. 48, no. 10, pp. D280-D298, 2009.

[6] Mason L. "Signal processing methods for non-invasive respiration monitoring," (Ph.D. thesis). University of Oxford, 2002.

[7] P. E. McSharry, G. D. Clifford, L. Tarassenko, and L. A. Smith, "A dynamical model for generating synthetic electrocardiogram signals," IEEE Trans. Biomed. Eng., vol. 50, no. 3, pp. 289-294, Mar. 2003.

[8] R.J. Cooper, L. Gagnon, D.M. Goldenholz, D.A. Boas and D.N. Greve, "The utility of near-infrared spectroscopy in the regression of low-frequency physiological noise from functional magnetic resonance imaging data," NeuroImage, vol. 59, pp. 3128–3138, 2012.

[9] T. E. Lund, K. H. Madsen, K. Sidaros, W. Luo, and T. E. Nichols, "Non-white noise in fMRI: Does modeling have an impact?," NeuroImage, vol. 29, pp. 54-66, 2006.

[10] M. Fabiani, K.A. Low, C.-H. Tan, B. Zimmerman, M.A. Fletcher, N. Schneider-Garces, E.L. Maclin, A.M. Chiarelli, B.P. Sutton and G. Gratton, "Taking the pulse of aging: Mapping pulse pressure and elasticity in cerebral arteries with optical methods," Psychophysiology, vol. 51, pp. 1072–1088, 2014.

[11] G. H. Glover, "Deconvolution of impulse response in event-related bold fMRI," NeuroImage, no. 9, pp. 416–429, 1999.

[12] M. A. Lindquist and T. D. Wager, "Validity and power in hemodynamic response modeling: A comparison study and a new approach," Human Brain Mapp., vol. 28, pp. 764-784, 2007.

[13] M. A. Kamran, M. Y. Jeong and M. N. M. Mannan, "Optimal hemodynamic response model for functional near-infrared spectroscopy," Front. Behav. Neurosci. vol. 9, June 2015.

[14] A. M. Chiarelli, E. L. Maclinb, M. Fabiani and G. Gratton, "A kurtosis-based wavelet algorithm for motion artifact correction of fNIRS data," NeuroImage, vol. 112, pp. 128–137, 2015.

ISBN 978-90-827970-1-5 © EURASIP 2018